

## Unveiling the Evolution of Type I AGNs in the IR ( $15\mu\text{m}$ ) — As Seen by ISO in the ELAIS-S1 Region

Israel Matute, Fabio La Franca

*Dipartimento di Fisica, Università degli studi "Roma Tre", Via della  
Vasca Navale 84, I-00146 Roma, Italy*

Carlotta Gruppioni, Francesca Pozzi, Carlo Lari

*Osservatorio Astronomico di Bologna, Via Ranzani 1, I-40127 Bologna,  
Italy*

**Abstract.** We present the first estimate of the evolution of type 1 AGNs in the IR ( $15\mu\text{m}$ ) obtained from the ELAIS survey in the S1 region. We find that the luminosity function (LF) of Type 1 AGNs at  $15\mu\text{m}$  is fairly well represented by a double power-law function with a bright slope of 2.9 and a faint slope of 1.1. There is evidence for significant cosmological evolution according to a pure luminosity evolution model  $L_{15}(z) \propto (1+z)^k$ , with  $k=3.00^{+0.16}_{-0.20}$  in a  $(\Omega_m, \Omega_\Lambda)=(1.0, 0.0)$  cosmology. This evolution is similar to what is observed at other wavebands. From the luminosity function and its evolution, we estimate a contribution of  $\sim 2\%$  from Type 1 AGN to the total Cosmic Infrared Background (CIRB) at  $15\mu\text{m}$ .

### 1. Introduction

In the past, AGN samples have been mainly selected in the optical and more recently in the soft-X with ROSAT. The first statistically significant samples of AGNs in the Infrared come from the IRAS mission. The lack of enough sensitivity for the IRAS satellite has limited these samples to objects in the local Universe ( $z \leq 0.1$ ). The evolution of the AGN population in the infrared could only be extrapolated from what was already known in the optical and X-ray.

The European Large Area ISO Survey (ELAIS) was carried out in order to extend to deeper fluxes the coverage of the luminosity-redshift space in the IR. This has given us the possibility to study the high redshift population ( $z \geq 0.2$ ), and allowed us to have the first insights on the evolution of IR selected sources.

### 2. The Sample: ELAIS-S1

The European Large Area ISO Survey (ELAIS) is the largest single open time project conducted by ISO (Oliver et al. 2000), mapping an area of  $12\text{ deg}^2$  at  $15\mu\text{m}$  with ISOCAM and at  $90\mu\text{m}$  with ISOPHOT. Four main fields were chosen

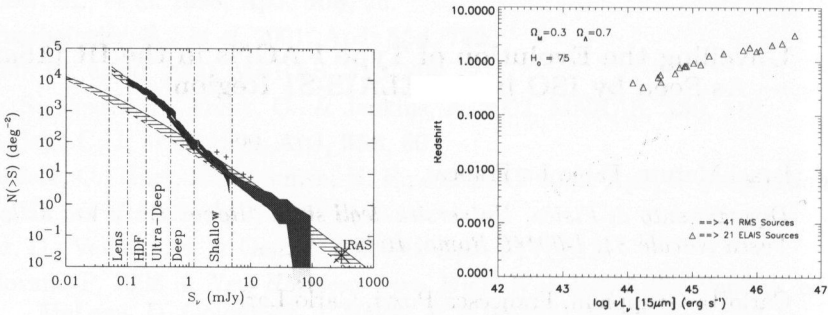


Figure 1. a) Integral Counts at  $15\mu\text{m}$  from the Final Analysis of the ELAIS-S1 Region (light grey shaded area). Also plotted are the faintest IRAS surveys and the deep ISOCAM surveys (dark grey shaded areas). b) The luminosity/redshift distribution of our 21 ELAIS-S1 and 41 RMS Type I AGNs that entered into the computation.

(N1, N2, N3 in the northern hemisphere and S1 in the south) due to their high Ecliptic latitudes ( $|\beta| > 40^\circ$ ) and low cirrus emission.

An initial catalog for S1 (J2000,  $\alpha : 00^{\text{h}}34^{\text{m}}44^{\text{s}}$ ,  $\delta : -43^\circ34'44''$ ), covering an area of  $3.96 \text{ deg}^2$ , was produced using the Imperial College data reduction technique (“Preliminary Analysis”, Serjeant et al., 2000). Optical identifications were possible thanks to an extensive R-band CCD survey, performed with the ESO 1.5m/Danish telescope. The spectroscopic follow-up program, carried out at the AAT at the AAO and the 3.6m/NTT at ESO/La Silla, of 114 sources in S1 fainter than  $R \sim 17.0$  provided the sample presented here.

The ELAIS-S1 field has also been completely covered in the radio at 1.4 GHz down to 0.3 mJy (Gruppioni et al., 1999), and 50% covered in the X-rays with BeppoSAX (Alexander et al., 2001). Now the Final Analysis has been completed by the ELAIS team in Bologna. The resulting complete catalog includes more than 450 sources, with fluxes at  $15\mu\text{m}$  down to 0.5 mJy and selected with  $S/N > 5$  (Lari et al., 2001).

For many years there has been a gap in flux between the brighter samples ( $>300 \text{ mJy}$ ), coming from the IRAS surveys and covering large sky areas, and the deep/pencil-beam surveys carried out by ISO at much fainter fluxes ( $<1 \text{ mJy}$ ). In the integral counts derived from the final analysis (Figure 4a, Gruppioni et al., in prep) we see how the ELAIS survey fills the whole flux range between these two regimes.

The nature of the objects identified by the spectroscopic follow-up is:

- High star-forming galaxies (45%);
- AGNs (Type 1 & 2) represent 30%;
- 15% of galaxies dominated by absorption lines;
- 4% of late-type stars;
- 6% of unclear classification (Type 2 AGN, Starburst, LINER).

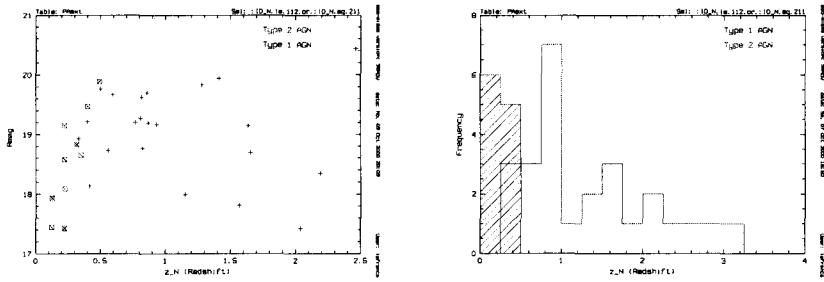


Figure 2. a) Distribution of Type I (plus symbols) and Type 2 (crossed squares) AGN in redshift-Rmag space. While the R-magnitude distribution is constant with a large spread for Type I AGN, Type 2 AGN show a trend with redshift, becoming fainter than  $R=20.0$  at  $z \sim 0.5$ . b) Distribution in redshift space of Type I AGN and AGN2 (shaded area). If we consider the redshift bin  $z=[0.0,0.5]$  the ratio of AGN2/Type I AGN becomes  $11/3 \sim 4$ .

Table 1. The percentages of all objects with emission lines

		type 1 AGN	type 2	ELG	LINERS
<b>ELAIS-S1</b>	%	20	10	50	2
15 $\mu$ m	$\langle z \rangle$	1.4	0.3	0.2	0.3
IRAS	%	6	17	54	23
12 $\mu$ m	$\langle z \rangle$	0.04	0.015	0.014	0.007

Note - IRAS subsample from Alexander & Ausserl (2000)

The observed ratio of the number of Type 2 with respect to Type 1+2 AGNs is 1/3. But this result is mainly an artifact due to the different selection functions of the sample for Type 1 AGN and Type 2 objects. The optical selection introduced in the spectroscopic follow-up ( $17.0 < R < 20.0$ ) seems to be the origin of the lack of Type 2 AGNs beyond  $z \sim 0.5$ . As a matter of fact, in Figure 2a a trend is observed for Type 2 with optical magnitudes being fainter at larger redshifts. In Figure 2b the redshift distributions of Type 1 and Type 2 AGN are shown. In the redshift bin where Type 2 AGNs are observed ( $z=0.0-0.5$ ), the ratio Type2/Type1 becomes  $\sim 4$ , similar to the predictions of the standard unification model. The follow-up campaign carried out in September/November 2001 with the ESO telescopes, and currently under study, will verify if this trend is seen at fainter and brighter optical fluxes.

### 3. The Evolution of Type I AGN

We have assumed  $H_0=75 \text{ km s}^{-1} \text{ Mpc}^{-1}$  and a  $(\Omega_m, \Omega_\Lambda)=(1.0, 0.0)$  cosmology. Our ELAIS preliminary sample of 21 Type 1 AGN is statistically significant enough to compute a first estimate of the evolution of these objects in the Mid-IR. The mean SED from Elvis et al. (1994) for radio quiet QSOs was adopted as a good representation of our sources.  $K$ -corrections in the IR were computed following Lang (1980) for each of the two different filters: ISOCAM-

LW3 at  $15\mu\text{m}$  and IRAS  $12\mu\text{m}$ .  $K$ -corrections in the R band were taken from Natali et al. (1998).

A subsample of Type 1 AGN was extracted from the catalog of Rush, Malkan & Spinoglio (1993) (RMS hereafter), as representative in the local universe of this type of object. The catalog consists of a sample of galaxies selected at  $12\mu\text{m}$  from the IRAS Point Source Catalog PSCv2 (Moshir et al. 1991), and is complete down to 0.3 Jy. With the computed  $K$ -correction,  $15\mu\text{m}$   $\nu L_\nu$  luminosities ( $L_{15}$ ) were derived. Figure 1b represents, in luminosity-redshift space, all Type 1 AGN coming from ELAIS and RMS that have been used in this analysis.

Similar to what was found in the optical (La Franca & Cristiani 1997; Boyle et al. 2000) and in the X-rays (Miyaji et al. 2000; La Franca et al. 2001 submitted), we adopted a smooth double power-law for the space density distribution of QSOs and Seyfert 1s in the local universe ( $z=0$ ):

$$\frac{d\Phi(L_{\text{IR}}, z=0)}{d\text{Log}L_{\text{IR}}} = \frac{\Phi^*}{\left[ (L_{\text{IR}}/L_*)^\alpha + (L_{\text{IR}}/L_*)^\beta \right]}$$

A standard pure luminosity evolution (PLE) has been adopted of the form  $L_{15}(z) = L_{15}(0)(1+z)^k$ . A parametric, unbinned maximum likelihood method was used to fit the evolution and luminosity function parameters simultaneously (Marshall et al., 1983) at  $15\mu\text{m}$ . Since ELAIS identifications were not only flux limited at  $15\mu\text{m}$ , but also in their R-band magnitude ( $17.0 < R < 20.0$ ), a factor  $\Theta(\mathbf{z}, \mathbf{L})$  was introduced in the function 'S' to be minimized

$$S = -2 \sum_{i=1}^N \ln[\Phi(z_i, L_i)] + \iint \Phi(\mathbf{z}, \mathbf{L}) \Omega(\mathbf{z}, \mathbf{L}) \Theta(\mathbf{z}, \mathbf{L}) \frac{dV}{dz} d\mathbf{z} d\mathbf{L},$$

to correct for incompleteness, and applied only to the ELAIS sample. This factor  $\Theta$  represents the probability that a source with a given luminosity at  $15\mu\text{m}$  ( $L_{15}$ ) has an R-magnitude ( $L_R$ ) between the limits of the sample ( $17.0 < R < 20.0$ ),

$$\Theta(\mathbf{z}, \mathbf{L}) (17.0 < R < 20.0 \mid L_{15}).$$

and was derived taking into account the  $1\sigma$  internal spread in the assumed SED.

From the total available list of Type 1 AGN of the sample, the number of objects that entered the computation was defined as:

- RMS: sources with  $F_{12\mu\text{m}} \geq 300$  mJy, 41 sources
- ELAIS: sources with  $F_{15\mu\text{m}} \geq 1$  mJy, and  $17.0 < R < 20.0$ , 21 sources

The resulting estimate of the LF of Type I AGN at  $15\mu\text{m}$  with its parameters is shown in Figure 3. The probability that our data have been drawn from the fitted PLE model is 0.28, as given by the 2D KS test. The PLE model adopted here could not be sufficient to represent the space density of our sources; some density evolution may be required. Currently we are studying different parameterizations taking into account some degree of density evolution.

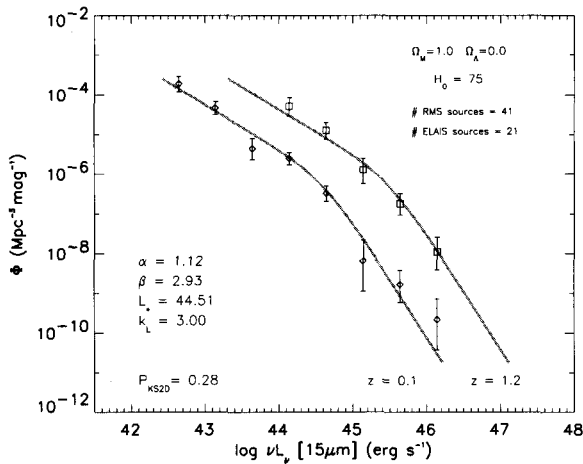


Figure 3. PLE fit to our 62 total sources (RMS + ELAIS-S1). The points correspond to the space densities of the observed sources, corrected for evolution within the redshift intervals. Sources with  $z=[0.0,0.2]$  are represented by diamonds and are mainly RMS sources. Sources with  $z=[0.2,2.2]$  are represented by squares, the ELAIS-S1 population. Lines plotted are the mid-LF at the central redshift of the interval considered. Also plotted are confidence levels at  $1\sigma$ .

For the derived PLE model the contribution of Type 1 AGN to the CIRB at  $15\mu\text{m}$  is  $\nu I_{\nu} = 5.2 \times 10^{-11} \text{ W m}^{-2}\text{sr}^{-1}$  which corresponds  $\sim 2\%$  of the lower limit to the CIRB calculated by Altieri et al. 1999 ( $\nu I_{\nu} = 3.3 \times 10^{-9} \text{ W m}^{-2}\text{sr}^{-1}$ ) in this band (see also Hauser & Dwek 2001; Hauser 2001). At maximum, the total contribution of AGNs to the background at  $15\mu\text{m}$  can be as high as  $\nu I_{\nu} = 2.6 \times 10^{-9} \text{ W m}^{-2}\text{sr}^{-1}$  ( $\sim 10\%$  of the background measured by Altieri et al. under the extreme assumptions: 1) that Type 2 AGN are as bright as Type 1 AGN at  $15\mu\text{m}$ , 2) that the ratio of Type 2 to Type 1 AGN is 4 at all redshifts, and 2) that Type 2 AGNs evolved with the same LF as Type I AGN.

#### 4. Conclusions

Thanks to the spectroscopic campaigns carried out on the ELAIS preliminary catalog in S1, we have been able to build up statistically significant samples of Type 1 AGNs and estimate the evolution of their LF in the IR.

Our sample of 21 Type 1 AGN has allowed the first estimate of this evolution at  $15\mu\text{m}$ , and their contribution to the Cosmic Infrared Background at that wavelength.

The LF is fairly well represented by a double power-law function with a significant cosmological evolution according to a PLE model with  $L(z) \propto (1+z)^k$  and  $k=3.00$ .

From the evolution fitted we can derive a total contribution, for Type 1 AGN, of around 2% to the total IR background as measured by Altieri et al 1999. The contribution of Type 1 + Type 2 AGNs could be as high as 10% if Type 2 AGNs evolve in a similar way to Type 1, and if we take the ratio  $\text{Type2}/\text{Type1} \sim 4$  and to be constant with  $z$ .

**Acknowledgments.** Based on observations collected at the European Southern Observatory, Chile, ESO N°: 62.P-0783, 63.O-0117(A), 64.O-0595(A), 65.O-0541(A). This research has made use of the NASA/IPAC Extragalactic Database (NED) which is operated by the Jet Propulsion Laboratory, California Institute of Technology, under contract with the National Aeronautics and Space Administration. This research has been partially supported by ASI contracts ARS-99-75, ASI 00/IR/103/AS, ASI I/R/107/00, MURST grants Cofin-98-02-32, Cofin-99-034, Cofin-00-02-36, and a 1999 CNA A grant.

## References

- Alexander, D., Aussel H. 2000, in the Springer Lecture Notes of Physics Series, ISO Surveys of a Dusty Universe, astro-ph/0002200
- Alexander, D., La Franca, F., Fiore, F. et al. 2001, *ApJ*, 554, 18
- Altieri, B., Metcalfe, L., Kneib, J.P. et al. 1999, *A&A*, 343, L65
- Boyle, B.J, Shanks T., Croom, S.M., Smith R.J., Miller L., Loaring N., Heymans C. 2000, *MNRAS*, 317, 1014
- Brandt, W.N., Alexander, D.M., Hornschemeier, A.E., et al., 2001., *AJ*, in press, astro-ph/0108404
- Elvis, M., Wilkes, B.J. et al. 1994, *ApJS*, 95, 1
- Grossan, B.A. 1992, PhD thesis, MIT
- Gruppioni, C. et al. 1999, *MNRAS*, 304, 199
- Hauser, M. G. 2001, in Proc. IAU Symposium 204, The Extragalactic Infrared Background and its Cosmological Implications, Astron. Soc. Pac. Conf. Ser., vol. 204, p. 101, astro-ph/0105550
- Hauser, M. G., Dwek, E. 2001, Annual Reviews of Astronomy and Astrophysics, 2001, Vol. 39, in press, astro-ph/0105539
- La Franca F., Cristiani S. 1997, *AJ*, 113, 1517
- Lari, C., Pozzi, F., Gruppioni, C. et al. 2001, *MNRAS*, 325, 1173
- Lang, K.R. 1980, *Astrophysical Formulae* (Berlin:Springer)
- Marshall, H.L., Avni, Y., Tananbaum, H., Zamorani, G. 1983, *ApJ*, 269, 35
- Miyaji T., Hasinger G., Schmidt M. 2000, *A&A*, 353, 25
- Moshir, M., et al. 1991, Explanatory Supplement to the IRAS Faint Source Survey, Version 2 (Pasadena:JPL)
- Natali, F., Giallongo, E., Cristiani, S. & La Franca, F. 1998, *AJ*, 115, 397
- Oliver, S., Rowan-Robinson, M., Alexander, D.M., et al. 2000, *MNRAS*, 316, 749
- Rush, B., Malkan, M.A., Spinoglio, L. 1993, *ApJS*, 89, 1 (RMS)
- Serjeant, S. et al. 2000, *MNRAS*, 316, 768